J. Physiol. (1979), **290**, *pp.* 227–252
With 11 *text-figures*
Printed in Great Britain

ELECTRICAL PROPERTIES ASSOCIATED WITH WIDE INTERCELLULAR CLEFTS IN RABBIT PURKINJE FIBRES

BY THOMAS J. COLATSKY AND R. W. TSIEN

From the Department of Physiology, Yale University School of Medicine, 333 Cedar Street, New Haven, Connecticut 06510, U.S.A.

(*Received 27 September 1978*)

SUMMARY

1. Rabbit Purkinje fibres were studied using micro-electrode recordings of electrical activity or a two-micro-electrode voltage clamp. Previous morphological work had suggested that these preparations offer structural advantages for the analysis of ionic permeability mechanisms.

2. Viable preparations could be obtained consistently by exposure to a K glutamate Tyrode solution during excision and recovery. In NaCl Tyrode solution, the action potential showed a large overshoot and fully developed plateau, but no pacemaker depolarization at negative potentials.

3. The passive electrical properties were consistent with morphological evidence for the accessibility of cleft membranes within the cell bundle. Electrotonic responses to intracellular current steps showed the behaviour expected for a simple leaky capacitative cable. Capacitative current transients under voltage clamp were changed very little by an eightfold reduction in the external solution conductivity.

4. Slow current changes attributable to K depletion were small compared to those found in other cardiac preparations. The amount of depletion was close to that predicted by a cleft model which assumed free K diffusion in 1 μm clefts.

5. Step depolarizations over the plateau range of potentials evoked a slow inward current which was resistant to tetrodotoxin but blocked by D600.

6. Strong depolarizations to potentials near 0 mV elicited a transient outward current and a slowly activating late outward current. Both components resembled currents found in sheep or calf Purkinje fibres.

7. These experiments support previous interpretations of slow plateau currents in terms of genuine permeability changes. The rabbit Purkinje fibre may allow various ionic channels to be studied with relatively little interference from radial non-uniformities in membrane potential or ion concentration.

INTRODUCTION

Studies of membrane currents in heart have been hampered by the structural properties of cardiac muscle preparations. Regardless of the voltage clamp technique used, it is clear that the morphology of cardiac tissue must introduce some degree of spatial and temporal nonuniformity (Johnson & Lieberman, 1971; Fozzard & Beeler, 1975; Attwell & Cohen, 1977). In many cardiac preparations, difficulties arise from the narrowness of spaces between adjacent cells. For example, the Purkinje

0022-3751/79/3200-0766 $01.00

fibres of ungulates such as sheep or calf have cleft spaces 20–40 nm wide (Sommer & Johnson, 1968; Mobley & Page, 1972; Hellam & Studt, 1974). During the flow of membrane current, ohmic voltage drops occur along the resistance of the cleft space and generate radial voltage non-uniformity. This non-uniformity can be tolerated for relatively small membrane currents (see for example, Kass, Siegelbaum & Tsien, 1978) but may be severe if the membrane current flow is intense. Narrow clefts also promote ion accumulation or depletion, and the associated changes in ionic driving force can interfere with the analysis of permeability mechanisms (Maughan, 1973; McGuigan, 1974; S. Noble, 1976; Baumgarten, Isenberg, McDonald & Ten Eick, 1977).

Purkinje fibres from the rabbit ventricle have been described by Harrington & Johnson (1973) as a 'naturally occurring preparation of cardiac muscle with the least undesirable morphology', appearing 'to have the minimum number of complexities and to be the closest approach to the ideal of a long cylindrical cell'. Johnson (1973) as a 'naturally occuring preparation of cardiac muscle with the wide except at localized regions of cell contact where the nexus was seen. Since the cleft width appears 25–50 times greater than in ungulate preparations, problems of radial series resistance and restricted diffusion should be much reduced. We tested these predictions by carrying out voltage clamp experiments with the two-microelectrode method. The electrical properties of rabbit Purkinje fibres were consistent with wide intercellular clefts. Effects due to radial voltage non-uniformity or K depletion were considerably smaller than those found in ungulate Purkinje fibres. Nevertheless, rabbit Purkinje fibres resembled the other preparations in showing slow plateau currents, including a slow inward current which was resistant to tetrodotoxin but blocked by the Ca channel inhibitor D600. These results favour the idea that the slow inward current and other time-dependent plateau currents reflect genuine changes in membrane permeability.

A preliminary report of this work has appeared (Colatsky, Siegelbaum & Tsien, 1978).

METHODS

Preparations

Most of the experiments were carried out in shortened Purkinje fibre bundles from rabbit hearts. This tissue runs freely between points of attachment to the walls of the left or right ventricle. In earlier work the preparation has been referred to as 'strand of cardiac muscle' or 'trabecula carnea' (Johnson & Sommer, 1967) or 'P fibre' or 'P strand' (Sommer & Johnson, 1968). The following structural features of the preparation were originally described by Sommer and Johnson and were supported by light and electron micrographs kindly taken by Mr Daniel Biemesderfer. In cross-section, the Purkinje fibre bundle consists of a cluster of two to twenty cells, with an individual diameter of about 10 μm. The cells lack transverse tubules. Adjacent cells are separated laterally by cleft spaces roughly 1 μm wide, except at occasional points of close apposition where nexuses may occur. The entire column of cells is surrounded by a layer of collagenous connective tissue, roughly 10 μm thick.

Adult rabbits weighing 3–10 lb. were killed by a sharp blow to the back of the head. The hearts were quickly removed, rinsed free of blood, and then placed in warm oxygenated potassium glutamate Tyrode solution (see below). After the hearts had relaxed from the high K contracture, the ventricles were carefully opened and short (0·5–1·8 mm) strands of Purkinje tissue were excised. Longer strands were sometimes seen but these were generally very thin and difficult to use in electrophysiological experiments. The excised preparations were incubated in K glutamate Tyrode solution for at least 30 min before exposure to the standard Na-containing Tyrode

solution. The exposure to K glutamate seemed to improve the eventual viability, probably by promoting healing-over (DeMello, 1972) and by preventing sodium loading (Barr, Headings & Bohr, 1962). Only preparations showing driven beats were used for the electrophysiological experiments. Initially, less than 10% of the preparations showed stimulated contractions, but this proportion increased to over 50% as we became more practiced in the dissection procedure. Preparations surviving the impalement with two micro-electrodes were remarkably stable; action potentials and good electrical coupling between cells could be observed for periods of 2–3 h.

In some experiments the rabbit preparation was compared to Purkinje fibres from calf hearts obtained from a local slaughterhouse. The calf Purkinje fibres were dissected in 4 mM-K, 5·4 mM-Ca Tyrode solution as in earlier work (Dudel *et al.* 1967; Tsien, 1974).

Experimental procedure

The experiments were carried out at 35–37 °C, with temperature held within ± 0·2 °C during an individual experiment. The composition of the standard Tyrode solution was as follows (mM): 150 NaCl, 4 KCl, 5·4 $CaCl_2$, 0·5 $MgCl_2$, 10 Tris-HCl (pH 7·2–7·4), 5 glucose. The solutions were pregassed with 100% O_2. In some experiments, 10 mM-HEPES was used instead of Tris but similar results were obtained. The dissections were carried out in a modified Tyrode solution in which all the NaCl and KCl was replaced by potassium glutamate, prepared by neutralizing glutamic acid (Sigma) with KOH. Some experiments employed a low conductivity bathing solution prepared by isosmotic substitution of sucrose for NaCl in the standard Tyrode solution. Measurements using a conductivity cell showed resistivities at 37 °C of 51 Ωcm (standard Tyrode solution) and 430 Ω cm (sucrose Tyrode solution).

Tetrodotoxin (TTX, Sankyo) and D600 (Knoll) were used in some experiments to inhibit components of inward current. In other studies, $CaCl_2$ was replaced by $SrCl_2$. Changes in the bathing K concentration were made by varying the amount of KCl without compensatory changes in other ion concentrations.

Membrane currents were recorded using the conventional two-microelectrode voltage clamp technique of Deck, Kern & Trautwein (1964) with the minor modifications described by Tsien (1974). Recordings of capacity current transients were improved by various means. The command pulse was lagged with an exponential time constant (usually 87 μsec) to reduce the peak current surge. Membrane potential was recorded differentially between intracellular and extracellular micro-electrodes. These were shielded to within 0·5 mm of their tips by a coating of Electrodag 416 (Acheson Colloids Co., Port Huron, MI.) and insulated with nail polish. The voltage electrodes' shields were driven and a similar shield around the current-passing electrode was grounded. Records of membrane potential and membrane current were taken with a chart recorder (Brush 440), a storage oscilloscope (Tekronix 5031 or 5103) and a laboratory computer (Digital Equipment Corp. PDP 8/e).

RESULTS

Resting and action potentials

This investigation began with micro-electrode recordings of electrical activity in short preparations. The viability of the isolated rabbit Purkinje fibre was a serious concern at the outset because of previous reports of low resting potentials and attenuated action potentials, both in the sucrose gap (Harrington & Johnson, 1973; Thompson, 1975) and with micro-electrode recording (Thompson, 1975). We found that fully polarized fibres could be obtained quite consistently as our dissection technique improved. Most of the preparations from each heart responded to external stimuli in an all-or-nothing fashion. The rabbit preparations with normal resting potentials often became partially depolarized after penetration by the second micro-electrode.

Fig. 1 illustrates the electrical activity seen in fully polarized (*A*) and partially depolarized preparations (*B*). Panel A shows action potentials evoked by external

stimuli. The membrane rises from a resting potential of −88 mV to an overshoot of +38 mV. Recording on a rapid time base shows a maximum rate-of-rise ($\dot{V}_{max}$) of 300 V/sec. The rapid depolarization phase is followed by a prominent secondary depolarization. The ensuing plateau was terminated by a final repolarization to the resting potential, with no undershoot or pace-maker depolarization. This recording typifies the behaviour of a group of fifteen preparations which remained fully polarized after satisfactory voltage impalements had been made. The collected results were as follows (mean ± S.E. of mean): resting potential, −83 ± 1 mV; plateau height,

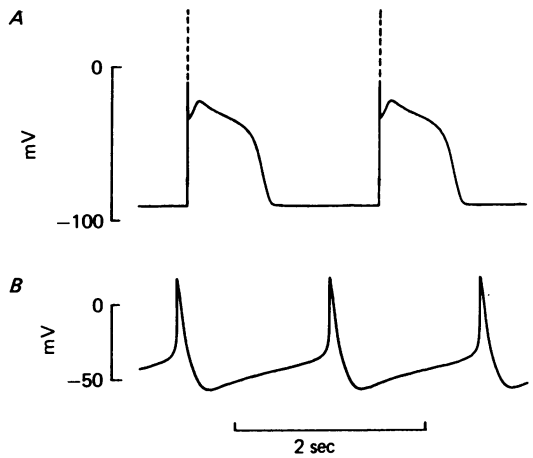

Fig. 1. Electrical activity in rabbit Purkinje fibres. *A*, action potentials evoked by external shocks at 0·5 Hz. Spikes were attenuated by chart recorder but dashed traces show true overshoot as recorded by oscilloscope. Preparation T23-1. *B*, spontaneous rhythmic activity in the form of 'slow responses' in a partially depolarized preparation. Preparation T09-1.

−22 ± 2 mV; action potential duration during steady 1 Hz stimulation, 645 ± 59 msec. Oscilloscope records of the upstroke were taken in six preparations and gave a collected value of +46 ± 4 mV for the overshoot. The upstroke velocity ($\dot{V}_{max}$) was 311 ± 37 *V*/sec in four preparations. The 'notch' formed by rapid repolarization and secondary depolarization was found in nine of fifteen preparations. Slow diastolic depolarization was absent in all but one case where a very slight depolarization (0·4 mV/sec) was observed.

These results are in good agreement with *in situ* recordings from rabbit Purkinje fibres in the intact ventricular wall (Johnson & Tille, 1961; Hoffman & Cranefield, 1960; Gibbs & Johnson, 1961; Tille, 1961). The earlier *in situ* action potentials also show secondary depolarizations and the appearance of a 'notch', although the overall action potential duration is briefer. The earlier recordings also show no pacemaker activity in fully polarized peripheral Purkinje tissue, although Hoffman & Cranefield (1960) did find phase 4 depolarization at more proximal locations in the bundle of His (see their Fig. 7–16). The virtual absence of pace-maker activity in fully polarized rabbit Purkinje fibres is the main electrical characteristic distinguishing them from sheep or calf Purkinje fibres, which regularly exhibit phase 4 depolarization (Draper

& Weidmann, 1951; Vassalle, 1966). In respect, the rabbit preparation may be similar to Purkinje fibres from several other species which have little or no diastolic depolarization under normal conditions (Hoffman & Cranefield, 1960, p. 176).

Pacemaker activity in partially depolarized fibres must be considered separately from diastolic depolarization in fully polarized tissue (see Noble, 1975). Fig. 1*B* shows spontaneous activity in a rabbit preparation that was partially depolarized by the insertion of the current micro-electrode. This type of activity has been referred to as 'slow response' (see Cranefield, 1975) because of its low rate-of-rise. It has also been termed 'low voltage oscillation' because of the range of potentials over which the activity occurs (Hauswirth, Noble & Tsien, 1969). In rabbit Purkinje fibres, as in other preparations, the slow response is associated with a visible contraction and can be abolished by the organic calcium channel inhibitor D600 (5 μg/ml.).

Linear cable properties

Fig. 2 shows an experiment where linear cable properties of the rabbit preparation were determined (cf. Weidmann, 1952; Fozzard, 1966). Small rectangular current pulses were introduced via an intracellular electrode approximately 360 μm from the end of a preparation (total apparent length, 1764 μm). Voltage changes resulting from the current flow were recorded at various impalement sites along the length of the fibre (inset). Responses *a* and *c* were determined individually, while responses *b* and *d* were obtained with simultaneous voltage recordings with two micro-electrodes. The preparation remained quiescent throughout the experiment with a resting potential of -84 mV.

Fig. 2*A* shows the steady voltage deflexions for a 15·8 nA current. These data were

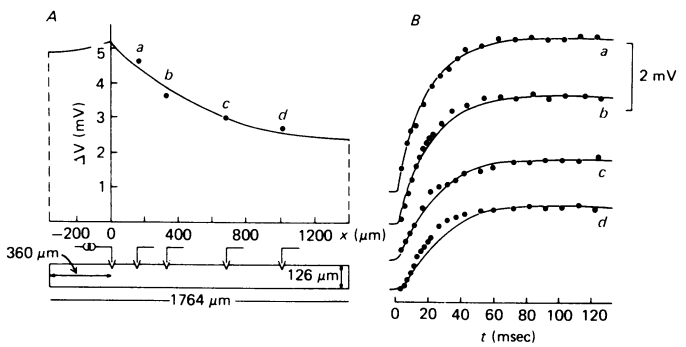

Fig. 2. Cable analysis of rabbit Purkinje fibre. *A*, steady-state electrotonic response to applied current. Inset shows fibre geometry and location of current-passing and voltage recording micro-electrode impalement sites. Responses *b* and *d* were recorded simultaneously during a 15·8 nA hyperpolarizing current pulse. Responses *a* and *c* were each recorded separately and have been corrected for small variations in the size of the current pulse. Resting membrane potential was -84 mV throughout. Smooth curve shows voltage distribution predicted for a cable with sealed ends and a longitudinal space constant of 1 mm. *B*, time course of experimental responses (points) and theoretical responses (continuous curves). The fit was obtained by setting the theoretical membrane time constant to 18 msec. To emphasize the temporal aspects of the comparison, small differences between experimental and theoretical steady-state values (shown in *A*) were suppressed by scaling the experimental points. The scaling factors for *a*–*d* were 0·96, 1·07, 1·0 and 0·94 respectively. Preparation T16-2.

compared with a theoretical curve for a one-dimensional cable with sealed ends (Weidmann, 1952). To the right of the current-passing electrode the curve is given by

$$V = V_0 \frac{\cosh (l-x)/\lambda}{\cosh (l/\lambda)}, \quad (1)$$

where l has been taken as the distance from the current-passing electrode to the visual end of the fibre (1404 μm) and λ the electrical length constant has been set a 1000 μm. The fit between the curve and the points is consistent with 'healing over' within a cell length of the cut end.

Fig. 2*B* shows the time course of the electrotonic response at the various impalement sites. The continuous curves are appropriate for the same theoretical cable as in *A* but with the membrane constant (τ) set at 18 msec. These curves were obtained by taking the Hodgkin-Rushton equation for an infinite RC cable and adding more terms for the 'reflections' at the sealed ends (see Jack, Noble & Tsien, 1975). Comparison between the theoretical and experimental time courses was carried out by slightly scaling each experimental transient so that its steady level at 200 msec coincided with the theoretical curve. From the close correspondence in *A* it is evident that the scaling factors were close to unity in each case.

All of the experimental results seem reasonably well fitted by the behavior of a simple RC cable. The largest deviation between data and theory was seen in record *d*, but the discrepancy was well within the noise on the voltage traces. Taking all four transients together, the fit would not have been significantly improved by replacing the simple RC membrane characteristic by a two time constant circuit (Falk & Fatt, 1964). In this sense, the rabbit Purkinje fibre differs from sheep preparations where the two time constant current is clearly superior (Fozzard, 1966; Freygang & Trautwein, 1970). The relatively simple behaviour of the rabbit preparation is consistent with rapid charging of the cleft membrane capacity (see Discussion).

Cable parameters were determined from the data in Fig. 2. The radius of the cell core was estimated from the external diameter by allowing for a connective tissue sheath 10 μm thick (Johnson & Sommer, 1967). From the values of λ, τ, V_0 and I_0 the following cable parameters were obtained: axial resistivity, R_i = 350 Ω cm; membrane capacity per unit apparent cylindrical surface, C_m = 13·6 μF/cm^2; membrane resistance per unit apparent cylindrical surface, R_m = 1·32 kΩ cm^2; assuming a specific capacity of 1 μF/cm^2, membrane resistance per unit membrane area R'_m = 18·0 kΩ cm^2. The values for C_m and R'_m from this experiment are not very different from those obtained for Purkinje fibres of other species (Weidmann, 1952; Fozzard, 1966; Freygang & Trautwein, 1970; Mobley & Page, 1972; Hellam & Studt, 1974; Schoenberg, Dominguez & Fozzard, 1975). The axial resistivity is higher than values given for sheep Purkinje fibres: 154 Ω cm (Coraboeuf & Weidmann, 1954) or 181 Ω cm (Weidmann, 1970), but is similar to R_i in working myocardium (see Discussion).

Capacity transients

Further analysis of passive cable properties was carried out in short rabbit Purkinje fibre preparations under voltage clamp. Fig. 3*A* illustrates the surge of capacitative current associated with a hyperpolarizing voltage step. The total capacity of the preparation was obtained from the area under the current surge after correction

for a small contribution of ionic current (Schneider & Chandler, 1976). In *A*, the total apparent capacity is 11·0 nF. When referred to the apparent fibre surface, this gives a total specific capacitance of 5·5 μF/cm^2. An average value of 6·5 $\pm$ 0·9 μF/cm^2 was obtained in a series of twelve rabbit preparations. We found a similar capacity in calf preparations, 6·6 $\pm$ 0·8 μF/cm^2 (n = 5). These values are somewhat smaller than the average capacity of a series of voltage clamped sheep Purkinje fibres, 9·4 μF/cm^2 (Fozzard, 1966) but the differences are not very striking in view of uncertainties in measurements of fibre geometry.

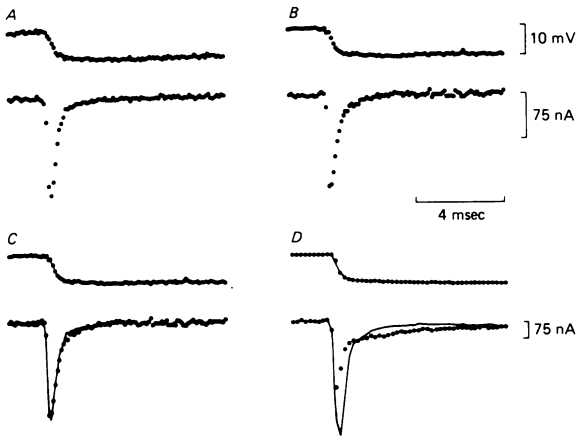

Fig. 3. Capacity transients from rabbit and calf Purkinje fibres in normal and low conductivity solutions. Traces are average of twelve sweeps. Upper traces are membrane potential; lower traces are current. Capacity currents were recorded from a rabbit Purkinje fibre in normal Tyrode solution (*A*) and 18 min after replacing all the NaCl with sucrose (*B*). These traces are superimposed in panel *C*, with the control records given as continuous lines. Preparation T17-2; holding potential -37 mV. Panel *D* presents similar data for calf Purkinje fibre. Preparation T20-1; holding potential -25 mV. The voltage command was exponentially rounded with a time constant of 125 μsec. 10 kHz filtering was used throughout.

The capacity current surge in Fig. 3*A* decays with a final exponential time constant of 0·49 msec. Since the decay phase outlasts the settling of the voltage signal, it is evident that the capacitative charging is limited by a series resistance of some kind. The simplest interpretation is that the series resistance arises from R_i, the resistance to longitudinal current flow within the preparation. This idea was pursued by seeing if the final time constant (τ_0) scales with fibre geometry in the manner expected if R_i were the only series resistance. Schoenberg, Dominguez & Fozzard (1975) have provided a theoretical analysis of the capacitative transient for a voltage step at one point in an RC cable with a sealed end. The final time constant of decay of the transient is given by

$$\tau_0 = \frac{\tau_m}{1 + (\pi^2/4)\,(\lambda/h)^2}. \qquad (2)$$

Here λ is the longitudinal space constant and h ($= l/2$) is the distance from the current passing electrode to either end of the preparation. Since $(\pi^2/4)\,(\lambda/h)^2 \gg 1$,

$\lambda^2 = aR_m/2R_i$ and $\tau_m = R_m C_m$, eqn. (2) reduces to

$$\tau_0 = R_i\left[C_m \frac{8}{\pi^2}\frac{h^2}{a}\right]. \quad (3)$$

This expression indicates that the final time constant should vary as (h^2/a) even if R_i is relatively constant from fibre to fibre. Results from seven preparations are given in Table 1. Fig. 4 plots τ_0 against the expression in brackets in eqn. (3). The

TABLE 1. Capacitance measurements from voltage clamp

Expt. no.	c_{tot} (nF)	a (μm)	$2h$ (μm)	C_m (μF/cm^2)	τ_0 (msec)	'R_i' (Ω cm)
S–1	10·0	45	1600	3·7	2·1	531
8–1	27·7	62	756	9·4	0·88	501
13–1	26·5	80	1080	4·9	0·57	394
17–2	11·0	44	720	5·5	0·49	369
24–1	15·4	52	864	5·5	0·71	445
26–1	8·1	52	900	2·8	0·42	486
32–1	17·2	35	1260	6·2	2·52	442
Mean	15·1	53	1026	5·4	1·10	453
± S.E. of mean	± 3·7	± 6	± 119	± 0·8	± 0·32	± 22

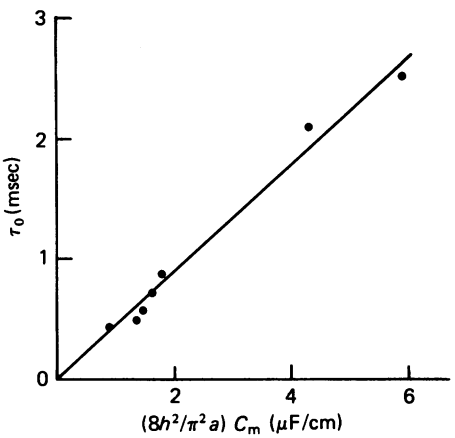

Fig. 4. Dependence of capacity transient time course on fibre geometry. τ_0, the time constant for the final decay of the capacity current, is plotted against $(8/\pi^2)$ (h^2/a) C_m for seven rabbit Purkinje fibre preparations. The straight line through the origin is predicted by a model in which charging of membrane capacity is rate-limited by longitudinal resistance. The slope of the line represents an apparent resistivity 'R_i' of 450 Ω cm and was chosen by eye to fit the points.

points fall close to a straight line through the origin, and are, therefore, consistent with the idea that τ_0 arises principally from longitudinal cable delay. The slope of the line corresponds to an apparent resistivity 'R_i' of 450 Ω cm. Individual estimates of 'R_i' ranged from 369 to 531 Ω cm (Table 1). These values are not much larger than 350 Ω cm, the estimate of R_i from the measurement of longitudinal decrement (Fig. 2). It appears than that longitudinal resistivity can largely account for τ_0. although a small component of external series resistance certainly cannot be ruled out.

Effects of reducing external solution conductivity

In the next series of experiments, possible sources of external series resistance were deliberately accentuated by decreasing the external conductivity. We looked for changes in the area or time course of the capacitative transient as the bulk solution conductivity was reduced 8·4-fold by isosmotic replacement of NaCl by sucrose. Fozzard (1966) first used this procedure in sheep Purkinje fibres and found a twofold increase in the late time constant of the capacity transient. Adrian & Almers (1974) observed a substantial fall in the effective capacity of frog skeletal muscle fibres when the T-system conductivity was decreased. Both sets of results are consistent with the development of significant radial voltage decrement along narrow clefts or T-tubules. If the clefts in the rabbit Purkinje fibre are as wide as 1 μm one might expect a different result since the radial space constant could decrease $\sqrt{8{\cdot}4}$ times and still remain large relative to the fibre radius.

Fig. 3 illustrates the effect of changing from NaCl-Tyrode (*A*) to the sucrose solution (*B*). The records in panel *B* were taken 18 min after the solution change, well after normal electrical responses were abolished by washout of extracellular sodium ions. Superposition of *A* and *B* (panel *C*) shows that the solution change produced no dramatic effect on the area of the capacitative surge. The apparent capacity fell from 11·0 nF in *A* to 10·7 nF in *B*, and recovered to 10·9 nF after restoration of NaCl Tyrode (record not shown). The ratio of the value in sucrose to the average of the bracketing control values is 0·98. In three other rabbit preparations, the corresponding ratio was 0·93, 0·95 and 0·96. Apparently, the radial space constant remains long relative to the fibre radius even after a substantial reduction in the conductivity of the cleft fluid.

Fig. 3*C* also shows relatively little change in the time course of the capacitative transient. Similar results were obtained in three other rabbit preparations. Fig. 3*D* illustrates the effect of the same change in bathing solution in calf Purkinje fibre. Here there is a roughly twofold increase in the final time constant, in good agreement with Fozzard's (1966) results in sheep preparations. Quantitative interpretation of small changes in the area or time course of the transients would be difficult without careful study of the influence of the solution changes on R_i and R_m. Nevertheless, the present results are in good qualitative agreement with expectations arising from the morphological studies on the rabbit preparation.

Cleft size and extracellular K depletion

The size of the extracellular cleft space is an important factor in determining the extent of extracellular ion concentration changes during membrane current flow. Considerable accumulation or depletion of K is expected if the extracellular space is small or if the endothelial layer is an appreciable diffusion barrier (see, for example, Frankenhaeuser & Hodgkin, 1956; Johnson & Lieberman, 1971; Barry & Adrian, 1973). It is not surprising, therefore, that membrane current changes associated with potassium concentration changes have been reported for frog myocardium (Maughan, 1973; S. Noble, 1976; Cleeman & Morad, 1976) sheep or calf ventricular muscle (McGuigan, 1974), rabbit atrium (Kunze, 1977) and sheep Purkinje fibre (Baumgarten & Isenberg, 1977). Variations in extracellular K are interesting because they may

contribute to persistent effects of electrical activity. However, they also create difficulties for the analysis of membrane permeability mechanisms.

Since morphological evidence indicates that rabbit Purkinje fibres have fairly wide clefts and a thin outer layer of connective tissue, it seems possible that these preparations might be relatively free from the complications of K accumulation or depletion. This prediction was tested by experiments of the type illustrated in Fig. 5. Strong hyperpolarizing pulses were used to drive inward potassium movement across cell membranes. A slow decline in the net inward current was taken as an indication of K depletion. Declining inward current is expected as the local potassium concentration falls since E_K shifts in the negative direction.

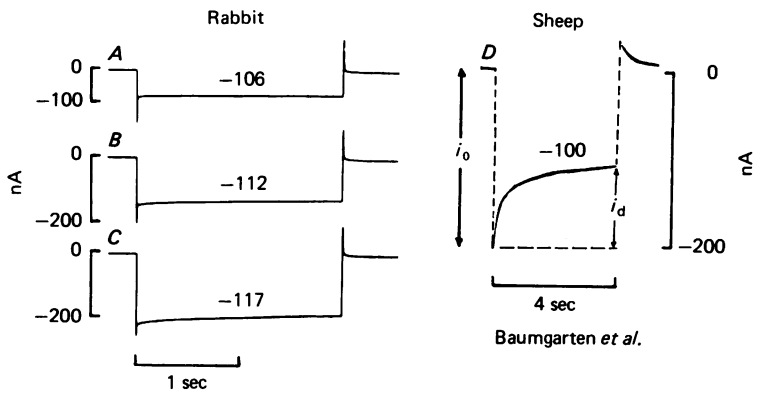

Fig. 5. Slow current changes attributable to K depletion during voltage clamp hyperpolarizations. *A–C*, rabbit Purkinje fibre. Current records associated with clamp pulses from a holding potential of −80 mV to the various levels indicated. The relative size of the depletion current during the hyperpolarizations was the largest found in six rabbit preparations. Preparation T27-5, 4 mM-K Tyrode solution. *D*, sheep Purkinje fibre. Current record associated with hyperpolarization from −89 to −100 mV in 5·4 mM-K Tyrode solution. Amplitude of the initial current jump (i_o) and slow depletion current (i_d) are indicated. From Baumgarten *et al.* (1977) with permission of the authors and the *Journal of General Physiology*.

Fig. 5*A-C* shows the clearest example of depletion current found in a total of six rabbit Purkinje preparations. The declining inward current is most evident in *C*, but depletion currents are present in *A* and *B* as well. For the sake of comparison, Fig. 5*D* shows an analogous experiment in a sheep Purkinje fibre (Baumgarten, Isenberg, McDonald & Ten Eick, 1977). Here the slow current change is quite obvious. Following the convention of Baumgarten *et al.*, the slow depletion current is designated i_d and the initial current immediately after the hyperpolarization is labelled i_0. Baumgarten *et al.*, used (i_d/i_0) as a measure of the severity of depletion and found values near 50% in Na-free solution. Baumgarten (personal communication) has found (i_d/i_0) between 30–35% for three sheep Purkinje fibres in Na-containing Tyrode solution. By the same criterion, the depletion is much less severe in rabbit Purkinje preparations: in records *A-C*, (i_d/i_0) was 12, 14 and 14% respectively. This was the worst case; an average value of 8 ± 3% was found in a total of six experiments.

Fig. 6 shows how the depletion current can be used to estimate the average fall in cleft K concentration. The estimate depends upon determining the current change due to a deliberate variation in the bathing K concentration, K_0. In this particular example, K_0 was changed from 4 to 2 mM. The membrane was clamped at a holding potential of -79 mV, a value close to the resting potential in both solutions. A hyperpolarizing step to -105 mV evoked the current records illustrated on the left side of the Figure. In 4 mM-K_0, (i_d/i_0) was 9%, a typical result for the series of

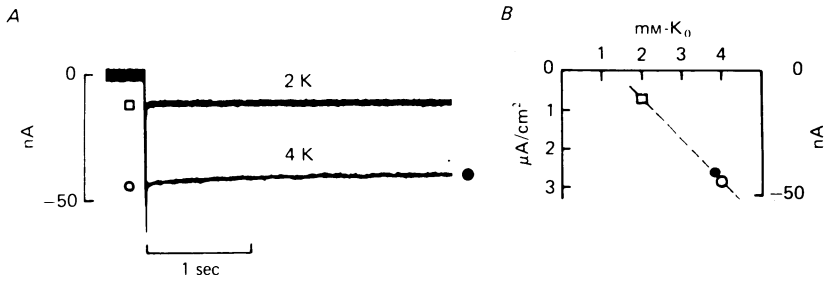

Fig. 6. Current changes due to hyperpolarization compared with current change produced by varying the external potassium concentration. *A*, superimposed records associated with hyperpolarization to -105 mV from a holding potential of -79 mV. Preparation T24-2, total capacitance, 15·4 nF. *B*, graphical interpetation of the experimental results. Initial currents at -105 mV in 4 mM-K (○) and 2 mM-K (□) are connected by a dashed line. The slope, -17 nA/mM, is an estimate of ($\mathrm{d}i/\mathrm{d}K$) near K = 4 mM. When plotted on the dashed line, the steady current after maintained hyperpolarization to -105 mV (●) gives a value of roughly 0·3 mM for the K depletion in a restricted extracellular space.

experiments. In 2 mM-K_0, the ratio was difficult to determine because both i_d and i_0 were small. Current levels indicated by the various symbols are plotted on the right hand graph and used to estimate the average potassium depletion, $\overline{\Delta K}$. According to the small-signal treatment of K depletion described in the Appendix:

$$i_d = \frac{A_c}{A_t}\left(\frac{di_o}{dK}\right)\overline{\Delta K}. \tag{15A}$$

The ratio of cleft area A_c to total area A_t was estimated as 0·81 (see Appendix). Using the slope of the dashed line in Fig. 6 as an approximate measure ($\mathrm{d}i_0/\mathrm{d}K$) at $K = 4$ mM, ($\mathrm{d}i_0/\mathrm{d}K$) is -17 nA/mM. The depletion current is 4 nA in the 4 mM record. Thus, from eqn. (15A),

$$\overline{\Delta K} = \frac{(4\text{ nA})}{(17\text{ nA/mM})\,(0{\cdot}81)} = -0{\cdot}29\text{ mM}.$$

This calculation is represented graphically in Fig. 6 with the simplification that the ratio of areas is taken as unity. As expected, $\overline{\Delta K}$ in the rabbit Purkinje fibre is small compared to estimates of K depletion in sheep Purkinje fibres. Using a different approach, Baumgarten *et al.* (1977) calculate that a prolonged 19 mV hyperpolarization would reduce the average cleft K from 5·4 to 3·4 mM.

Radial distribution of K and depletion current predicted from a simple cleft model

The next question is whether the size of the observed depletion current is quantitatively consistent with the observed morphology of rabbit Purkinje fibres (Johnson & Sommer, 1967; Sommer & Johnson, 1968). We approached this question by developing a model for the radial distribution of K within the clefts. The Appendix presents the mathematical treatment and points out its resemblance to standard one-dimensional cable theory. Fig. 7 summarizes some of the main results. The inset

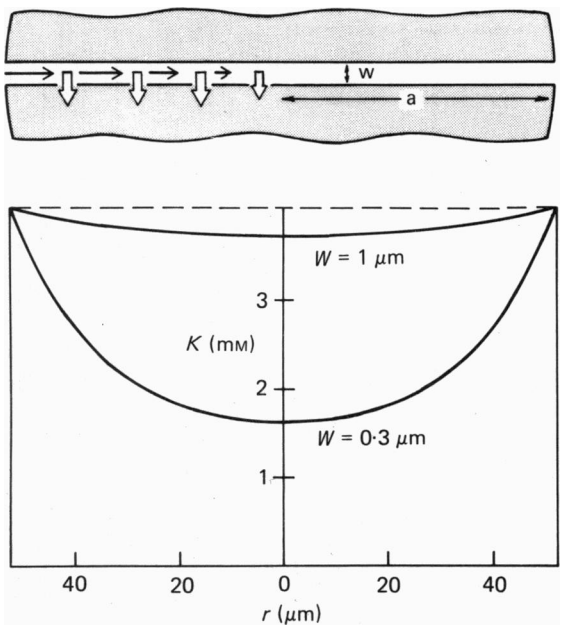

Fig. 7. Predicted K profiles for linear model of K depletion in clefts. Inset shows idealization of cleft geometry. During maintained hyperpolarization, cleft K reaches a steady state where radial diffusion (filled arrows) balances inward fluxes across the cleft membrane (open arrows). Graph plots steady-state profile predicted by eqn. (9*A*) for cleft widths of 1 μm and 300 Å. For further details, see Appendix.

shows a simplified view of a cleft, and indicates schematically the steady-state balance between inward diffusion along the cleft (thin filled arrows) and inward transmembrane flux (open arrows). The lower panel shows a predicted K profile for the rabbit Purkinje fibre (cleft width $w = 1$ μm). For the 1 μm theoretical cleft, the model predicts a diffusional space constant λ_K of about 100 μm. This gives rise to a maximum depletion of 0·32 mM at the centre of the fibre and an average depletion $\overline{\Delta K}$ of 0·21 mM. This prediction for $\overline{\Delta K}$ is not very different from 0·29 mM, the $\overline{\Delta K}$ estimated from experimental results without assumptions about cleft geometry. The comparison between cleft model and experiment can also be expressed in terms of the relative size of the depletion current. For the 1 μm wide cleft, the predicted (i_d/i_0) was 6·5% (see Appendix) while the observed values was 8·8%. Stated either way,

the agreement between model and experiment seems consistent with the assumption of free K diffusion in 1 μm clefts.

Fig. 7 also shows the predicted K profile for a cleft 300 Å wide but with otherwise identical parameters. The predicted values of $\overline{\Delta K}$ = 1·77 mM, and (i_d/i_0) = 54% are close to experimental findings in sheep Purkinje fibres (Baumgarten *et al.* 1977). The agreement should be viewed with caution since the calculation assumes similar properties for i_K in rabbit and sheep and since the linear treatment becomes more approximate as depletion grows larger.

Slow inward current (I_{si})

The results from our electrical experiments seem entirely consistent with the earlier morphological evidence for wide clefts. Both approaches suggest that the rabbit Purkinje fibre has a favourable structure for minimizing interference from

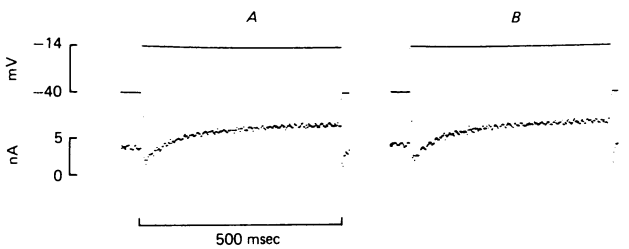

Fig. 8. Lack of effect of tetrodotoxin on slow inward plateau current in rabbit Purkinje fibres. Currents were recorded before (*A*) and after (*B*) the addition of 20 μM-TTX to the Tyrode solution. Membrane potential was stepped from −40 to −14 mV for 500 msec. Sr replaced Ca in the Tyrode solution to minimize the transient outward current (see text). Preparation T26-1.

nonuniformities of membrane potential or ion concentration during the study of ionic currents. Voltage clamp experiments in the rabbit preparation have already been carried out by Harrington & Johnson (1973) and Thompson (1975), Using the double sucrose gap technique, these investigators found no time-dependent ionic currents other than a tetrodotoxin-sensitive Na current, I_{Na}. Since they failed to observe a distinct 'secondary' or 'slow' inward current, one might argue that in other preparations with less favourable geometry, slow inward current arises from poor voltage control of I_{Na}. However, the absence of I_{si} could also be attributed to the double sucrose gap procedure. It seemed worthwhile, therefore, to see if slow inward current could be observed with another voltage clamp technique.

Using the two-micro-electrode method, we found that rabbit Purkinje fibres show slow inward current rather consistently. The slow inward current was identified by its time course and by its resistance to TTX and sensitivity to D600. Fig. 8 illustrates an experiment where the slow inward current was accentuated by using strontium in place of Ca in the external solution (Vereecke & Carmeliet, 1971). The membrane potential was held at −40 mV to inactivate I_{Na} (Weidmann, 1955). In *A*, a step depolarization to −14 mV evoked a slow inward current which peaked early and then slowly delined. Panel *B* shows that the slow inward current was not affected by tetrodotoxin at a concentration (20 μM) sufficient to block normal excitability. Such TTX

resistance is characteristic of slow inward currents found in other cardiac preparations (see Reuter, 1973).

Fig. 9 illustrates the effect of the drug D600, which blocks inward calcium movements in a variety of excitable cells (see Fleckenstein, 1977 for review). In this experiment, the external solution contained the usual 5·4 mM-Ca. The slow inward current observed in a control run (*A*) was abolished by exposure to 5×10^{-6} g/ml. D600 (*B*). The D600-sensitive current is given as the difference signal (*A*-*B*). The drug-sensitive current shows a significant maintained component, as in calf Purkinje fibres (Kass, Siegelbaum & Tsien, 1976).

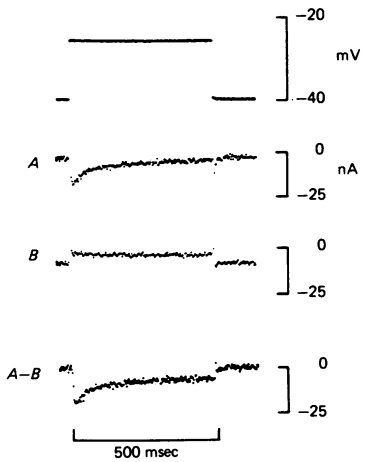

Fig. 9. Effects of D600 on the slow inward current. Plateau currents were recorded in normal Tyrode solution (*A*) and in the presence of 5 μg/ml. D600 (*B*); holding potential -40 mV. The lower tracing (*A*-*B*) is the D600-sensitive current obtained by subtracting traces *A* and *B*. Preparation T08-1.

These experiments indicate that the slow inward current can be observed in rabbit Purkinje fibres and that its properties appear similar to those reported for other cardiac preparations. The presence of I_{si} seems compatible with recording of slow responses or prominent secondary depolarizations preceding the plateau (Fig. 1). Our results differ from those of Harrington & Johnson (1973) and Thompson (1975) but the discrepancy may be explained by differences in experimental technique (see Discussion).

Time-dependent outward currents

The similarity between rabbit preparations and ungulate Purkinje fibres extends to outward currents activated over the plateau range of potentials. Fig. 10 shows an experiment in which a prolonged depolarizing clamp pulse to -3 mV elicited two outward components. The first component was a transient outward current which peaked early and declined within a hundred milliseconds. There is also a late increase in outward current which seems to be correlated with the development of outward current tails following repolarization to the holding potential.

The transient outward current has been studied previously in sheep Purkinje

fibres. It is triggered by depolarizations beyond − 20 mV and helps generate the rapid early repolarization following the crest of the action potential (Dudel, Peper, Rudel & Trautwein, 1967; Reuter, 1968; Fozzard & Hiraoka, 1973). Kenyon & Gibbons (1979) have found that the transient outward current is inhibited by tetraethylammonium or 4-aminopyridine, and have suggested that the outward current was carried by potassium ions. Baumgarten *et al.* (1977) also considered the possibility of a K efflux, and suggested that the 'inactivation' might be generated by K accumu-

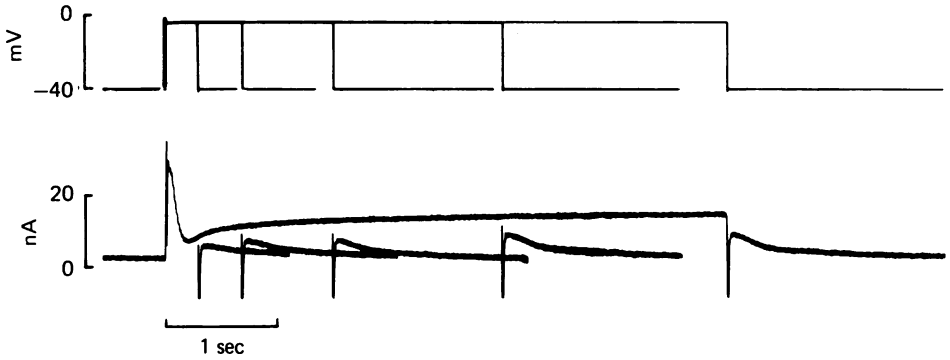

Fig. 10. Outward plateau currents in rabbit Purkinje fibres. Delayed rectifier and transient outward currents elicited by depolarization to − 26 mV from a holding potential of − 40 mV. The duration of the clamp step was varied from 300 to 4950 msec. Preparation T24-2.

lation in the sheep Purkinje fibre clefts. The present results do not favour K accumulation as a general explanation of inactivation since the time course of decline is similar while K equilibration seems relatively unrestricted.

The late outward current and associated tail currents in Fig. 10 resemble the current I_x in sheep Purkinje fibres (Noble & Tsien, 1969). I_x has also been attributed to K accumulation in narrow clefts of the sheep preparation (see, for example, Johnson & Lieberman, 1971). Such an explanation is difficult for the case of the rabbit Purkinje fibre because so little depletion is evoked by relatively large hyperpolarizing currents. The rabbit preparation seems promising for future analysis of outward plateau currents.

Unlike sheep or calf Purkinje fibres, the rabbit preparations do not show slow current changes characteristic of the pacemaker K current, I_{K_2} (Vassalle, 1966; Noble & Tsien, 1968). The absence of pacemaker current changes is not readily explained by the dissection or voltage clamp procedures since earlier recordings show a corresponding lack of I_{K_2}-dependent pacemaker activity in peripheral Purkinje tissue *in situ* (p. 230). The apparent lack of I_{K_2} is particularly intriguing because of the anatomical differences between rabbit and ungulate preparations. However, the correlation between wide clefts and the lack of I_{K_2} may be fortuitious; we know of no convincing explanation of I_{K_2} in terms of ion concentration changes alone.

Arrhythmogenic phenomena

Since 1973 there has been considerable interest in a special kind of pace-maker activity found in Purkinje fibres intoxicated with digitalis or exposed to high external Ca (see Ferrier, 1977 or Tsien & Carpenter, 1978 for review). Typically, a series of closely spaced action potentials is followed by an oscillatory afterpotential (a so-called 'transient depolarization') which can reach threshold and produce an ectopic impulse. Voltage clamp experiments show that the transient depolarization is

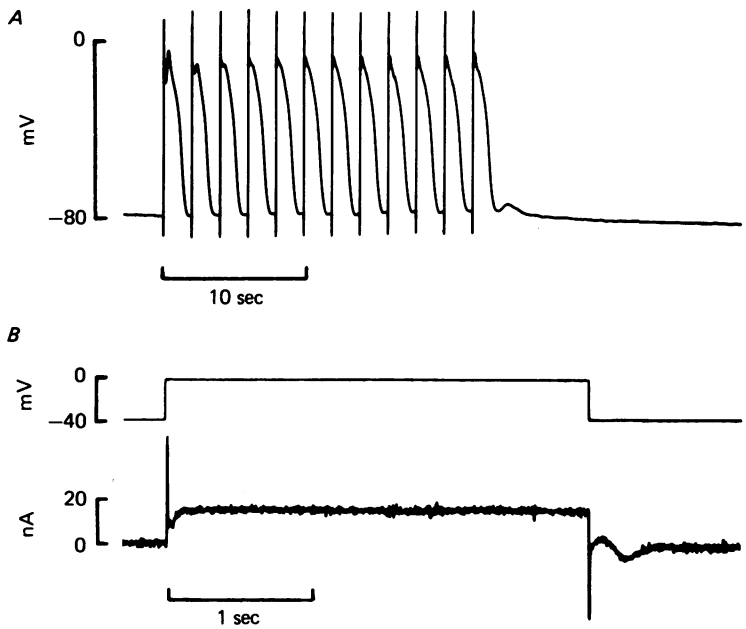

Fig. 11. Transient voltage and current oscillations in rabbit Purkinje fibres. *A*, spontaneous subthreshold depolarization following a train of twelve action potentials; stimulus rate 0·5 Hz. Preparation T08-1. *B*, transient inward current evoked by a 3 sec depolarizing voltage clamp step; holding potential −40 mV. Preparation T16-1.

generated by a transient inward current with an oscillatory waveform (Lederer & Tsien, 1976; Aronson & Gelles, 1977). Cohen, Attwell & Eisner (personal communication) have hypothesized that the arrhythmogenic current is generated by an oscillation in the K concentration of a restricted extracellular space. However, as Fig. 11 illustrates, the transient depolarization or transient inward current can be observed in rabbit Purkinje fibres, despite the relatively unrestricted diffusion of extracellular K. The timing of the transient depolarization (*A*) or transient inward current (*B*) is quite similar to that found in Purkinje fibres with narrow clefts. These results are consistent with observations of spontaneous oscillations in membrane current and contraction in enzymatically isolated dog Purkinje cells (Mehdi & Sachs, 1978). Evidently, changes in extracellular K are not a primary factor in the oscillatory mechanism. Other lines of evidence indicate that the oscillatory mechanism involves variations in intracellular calcium (Kass, Lederer, Tsien & Weingart, 1978).

DISCUSSION

Comparisons between electrical and morphological observations

Our results provide experimental support for earlier suggestions about the advantages of the rabbit Purkinje fibre as an electrophysiological preparation (Johnson & Sommer, 1967; Harrington & Johnson, 1973). The electrical properties of intact preparations are consistent with the structural features seen with light or electron microscopy on fixed tissue.

Cable properties. Electrotonic responses to current steps agreed in both magnitude and time course with theoretical curves for a cable with a single membrane time constant and sealed ends. Within the resolution of the micro-electrode impalements, the preparation behaves as a simple leaky capacitative cable. This finding is not in conflict with Johnson & Sommer's (1967) light microscope study of lateral 'occlusions' between adjacent cells in a rabbit Purkinje fibre bundle. They found considerable variability in the incidence of 'occlusions' but the observations were made over a 200 μm stretch, which is short relative to the DC space constant (roughly 1 mm). Furthermore as Johnson & Sommer point out, 'occlusions' indicate junctional complexes, but only provide a lower limit on the actual number of nexal connexions.

Estimates of axial resistivity of the cable (R_1) were obtained from the longitudinal space constant or from the final time constant of the capacitative transient in voltage-clamped preparations. The values ranged from 350 up to 530 Ω cm. These values are higher than estimates for ungulate Purkinje fibres, but they are similar to Weidmann's (1970) estimate of R_1 in ventricular muscle, 470 Ω cm. The resemblance to ventricular muscle can be interpreted in terms of myoplasmic or nexal properties or both. Rabbit Purkinje fibres are densely packed with myofibrillar material (Johnson & Sommer, 1967), like ventricular muscle but unlike ungulate Purkinje fibres. Alternatively, nexal contacts may be less frequent in the rabbit Purkinje fibre than in ungulate preparations. Future morphometry may show whether the rabbit Purkinje fibre resembles rabbit papillary muscle, where nexuses occupy 0·017 $\mu m^2/\mu m^3$ cell volume (Page, 1978) or sheep Purkinje fibre, where the corresponding value is 0·066 $\mu m^2/\mu m^3$ (Mobley & Page, 1972, p. 556).

Capacitative transients under voltage clamp. The bathing solution conductivity was reduced eightfold in an effort to analyse possible barriers to radial current flow. The decrease in conductivity produced very little change in either the magnitude of the effective capacitance (Adrian & Almers, 1974) or the time course of the capacitative current transient. In this respect, the rabbit Purkinje fibre differs from Purkinje fibres of sheep (Fozzard, 1966) or calf (Fig. 4*D*) or frog skeletal muscle (Adrian & Almers, 1974). The results in rabbit preparations are to be expected if the clefts are in fact 1 μm wide. Theoretical estimates of the radial space constant λ_c can be made by assuming that the cleft fluid has the resistivity of NaCl Tyrode (51 Ω cm) or sucrose Tyrode (430 Ω cm). Using eqn. (11A) and a membrane resistance R'_m of 18 kΩ cm^2, λ_c = 1328 μm for NaCl Tyrode and λ_c = 457 μm for sucrose Tyrode. In either case, the space constant is much greater than the fibre radius, so little radial voltage decrement or attentuation of effective capacitance should occur. Calculations of the final time constant for charging the cleft capacitance can be made using the approach of Schoenberg *et al.* (1975). For a 1 μm wide cleft, the estimated final time constant is

10 μsec in NaCl Tyrode and 84 μsec in sucrose Tyrode. These values are fast relative to the estimated time course of longitudinal current spread even in relatively short preparations. It is reasonable, therefore, that a clear change in capacitative current time course was not seen when the external conductivity was varied.

K depletion currents. Hyperpolarizing voltage steps evoked small but clear current changes of the type expected for K depletion in the cleft space. The size of the depletion current was in good agreement with that predicted for free diffusion of K in a cleft 1 μm wide. This is perhaps the most critical comparison between electrical and morphological observations.

Our treatment of the depletion problem emphasizes the qualitative analogy between the radial distributions of potential and K concentration. However, the depletion experiment is much more sensitive to morphological limitations than the measurements of effective capacitance, because the diffusional space constant is much smaller than the electrical space constant in the radial direction. Radial non-uniformities in concentration occur more readily because of the disparity in the potassium transport numbers of the cleft membrane and the cleft fluid. In view of the sensitivity of the depletion current measurement, it would be interesting to look for depletion currents in cultured cardiac preparations (Lieberman, Sawanobori, Kootsey & Johnson, 1975, Sachs, 1975) when comparing them to the rabbit Purkinje fibre.

Connective tissue sheath as diffusion barrier. The radial pathway for K diffusion or current flow traverses a 10 μm thick connective tissue layer which lies in series with the clefts. Elsewhere in the paper, attention has been focused on the possible effects of the cleft spaces. The outer layer of endothelial cells or other elements of the connective tissue sheath were ignored because the main goal was a minimum estimate of the cleft width under electrophysiological conditions. This approach seemed justified since estimates of cleft width from the depletion results would only be increased if an additional diffusion barrier were considered.

It is also useful to consider the other extreme case, in which the diffusion barrier is attributed to the connective tissue sheath alone. In this case, the diffusional properties of the clefts are completely ignored, as though the clefts were much wider than 1 μm, and the depletion currents are used to calculate a lower limit on the sheath potassium permeability, $P_{K,S}$. Applying Fick's law to the sheath in the steady-state,

$$P_{K,S}(K_o - K_a) = \left|\frac{I_K}{F A_s}\right|. \tag{4}$$

Here K_a is the K concentration just inside the sheath and A_s is the sheath area. K_a is not known but (K), the average K concentration seen by the cell membranes, can be estimated from the procedure described on p. 237. For inward K diffusion, $(K_o - (K)) = \Delta K > (K_o - K_a)$. Thus, eqn. (4) may be reexpressed as an inequality,

$$P_{K,S}\,\Delta K > \left|\frac{I_K}{F A_s}\right|. \tag{5}$$

For the experiment illustrated in Fig. 5, the steady inward current (predominantly K) is 40 nA, $A_S = 3{\cdot}37 \times 10^{-3}$ cm^2 and $|\Delta K| = 0{\cdot}35$ mM. Thus,

$$P_{K,S} > 3{\cdot}5 \times 10^{-4} \text{ cm/sec}.$$

This lower limit in K permeability can be converted into a maximum estimate of series resistance R_s (cf. Frankenhaeuser & Hodgkin, 1956). The permeability $P_{K,S}$ is related to the diffusion coefficient in free solution by $P_{K,S} = D_K A/L$, where L is the effective thickness and A represents the degree to which diffusion is restricted. Assuming that the same factor A applies to current flow, $R_s = \rho (A/L)^{-1}$ where ρ is the resistivity of Tyrode solution. Combining these expressions with eqn. (5) gives

$$R_s < \frac{\rho D_K}{P_{K,S}} = \frac{(50\ \Omega\ \text{cm})\ (2{\cdot}3 \times 10^{-5}\ \text{cm}^2\ \text{sec}^{-1})}{(3{\cdot}5 \times 10^{-4}\ \text{cm sec}^{-1})} = 3{\cdot}3\ \Omega\ \text{cm}^2. \quad (6)$$

This value is considerably lower than an estimate of $R_s = 40\ \Omega\ \text{cm}^2$ in frog ventricular trabeculae, made by Attwell & Cohen (1977) from morphological data of Page & Niedergerke (1972). The present limiting value falls close to the series resistance of squid giant axons as determined by Frankenhaeuser & Hodgkin (1956) from electrical measurements or considerations of potassium permeability. A low value of R_s in the rabbit Purkinje fibre would be favourable for future studies on the rapid excitatory Na current.

The external series resistance has been estimated in other cardiac preparations using either the peak amplitude (Connor *et al.* 1975; Attwell & Cohen, 1977) or time course (Beeler & Reuter, 1970; Johnson & Lieberman, 1971) of the capacity transient. These approaches would not be appropriate for the rabbit Purkinje fibre because the internal longitudinal resistance greatly overshadows the resistance of the clefts and connective tissue sheath.

Ionic currents

Time-dependent plateau currents in the rabbit Purkinje fibre appeared similar to those reported for preparations with less favourable electrical structure. Step depolarizations from -40 to about -20 mV evoked a slow inward current carried by divalent cations (I_{si}) which was characterized by its time course of inactivation, resistance to TTX and sensitivity to D600. Depolarizations beyond -10 mV or so evoked a transient outward current which partially or completely obscured I_{si}. When a strong depolarization was maintained, outward current slowly increased as a result of a conductance system with a reversal potential near -75 mV. The slow inward current and the transient and delayed outward currents were small compared to the hyperpolarizing current needed to produce clearcut K depletion in the same experiments. All three components were similar to currents found earlier in sheep or calf Purkinje fibres (see McAllister *et al.* 1975 for review). Their presence in the rabbit Purkinje fibre supports the view that the slow plateau currents reflect genuine permeability changes, not merely non-uniformities of membrane potential or ion concentration.

Slow plateau currents were not reported in earlier studies of the rabbit Purkinje fibre by Harrington & Johnson (1973) or Thompson (1975). Their use of the double sucrose gap may help explain the discrepancy. In the double sucrose gap, the rabbit preparations were partially depolarized and only gave regenerative responses after a hyperpolarizing current pulse. The responses were triangular and lacked the fully developed plateau seen with micro-electrode recordings from Purkinje fibres *in situ* (Hoffman & Cranefield, 1960; Johnson & Tille, 1961; Gibbs & Johnson, 1961) or isolated preparations (this paper). The I–V relations in the sucrose gap (Harrington

& Johnson, 1973) showed a large linear 'leak' with no evidence of the inward rectification we observed with the two-micro-electrode voltage clamp (data not shown). Both the triangular action potential and the 'leak' component can be attributed to transmembrane current flow in the sucrose regions (deHemptinne, 1973; McGuigan & Tsien, appendix to McGuigan, 1974). Such shunt currents could easily have swamped slow plateau currents from the narrow test nodes used by Harrington & Johnson and Thompson. The membrane area in a 40–60 μm test node (Thompson, 1975) is roughly twentyfold smaller than the area of the preparations we used. Slow currents 20 times smaller than those shown in this paper could easily have been missed at the low current amplification used in the double sucrose gap experiments.

The experiments described in this paper provide electrical evidence that the rabbit Purkinje fibre has simple morphology compared to other cardiac preparations. The absence of serious non-uniformities in membrane potential and ion concentration holds promise for future voltage clamp studies of membrane currents including the fast Na current.

APPENDIX

Radial distribution of K in the cleft space

Radial nonuniformity of potassium in the clefts is described by a simple model which starts with a morphological estimate of cleft width (Johnson & Sommer, 1967) and an electrical estimate of membrane current density. It predicts the radial distribution of cleft K during a steady hyperpolarization and the magnitude of the associated depletion current. The analysis is similar in some ways to numerical simulations of the K profile in the T-system of skeletal muscle (Barry & Adrian, 1973) or in the 'intercalated disk clefts' of heart muscle (MacDonald, Hsu, Mann & Sperelakis, 1975). In the present case the predicted K distribution can be given analytically by an expression equivalent to an electrical cable equation.

Our treatment takes advantage of the relatively simple properties of the rabbit Purkinje fibre. First, radial diffusion is treated as a one-dimensional problem since the clefts resemble spokes of a wheel (Sommer & Johnson, 1968; Hellam & Studt, 1974; Schoenberg *et al.* 1975) rather than a fine uniform mesh as in the T-system of skeletal muscle. Secondly, the cleft space is treated as isopotential since the electrical space constant is much larger than the fibre radius (see p. 217). Finally, it is assumed that the cleft membrane current varies linearly with cleft K for small perturbations in concentration.

Fig. 7 shows the basic features of the model. The cleft space is assigned a constant width (w) and a uniform diffusivity for K (D). D is taken as the diffusion coefficient for K in bulk solution at 37 °C, $2{\cdot}3 \times 10^{-5}$ cm^2 sec^{-1} (Weidmann, 1966). The cleft extends from the axis of the bundle ($r = 0$) to the edge ($r = a$). Tortuosity, branching and membrane folding are neglected in the absence of morphometric information for the rabbit preparation. Membrane properties are presumed to be evenly distributed throughout the total cell surface; membrane current density is calculated from a total area (A_t) inferred from total preparation capacity and a specific capacity of 1 μF/cm^2. The potassium concentration within the clefts is designated $K(r)$

while the bulk potassium concentration is K_0. The net radial flux of K (M) is driven by the concentration gradient according to Fick's law:

$$M = -D\frac{dK}{dr}. \tag{1A}$$

This equation ignores movement of K due to radial current flow *per se* since the transport number of K in the external fluid is close to zero. Now let J_K be the net transmembrane potassium current density due to either passive or active transport. By convention, J_K is positive for current leaving the cell. Using the equation of continuity for the steady-state case,

$$w\frac{dM}{dr} = \frac{2}{F}J_K. \tag{2A}$$

F is the Faraday and the factor of 2 reflects the presence of a pair of membranes bounding the cleft space. Combining (1A) and (2A) gives

$$\frac{d^2K}{dr^2} = -\frac{2}{wFD}J_K. \tag{3A}$$

This equation can be re-expressed in terms of a perturbation in cleft K, ΔK, relative to the resting condition where $K(r) = K_0$. Substituting $K = K_0 + \Delta K$, in (3A),

$$\frac{d^2\Delta K}{dr^2} = -\frac{2}{wFD}J_K. \tag{4A}$$

The boundary conditions are as follows. Since there is no radial flux at the fibre axis,

$$\left(\frac{d\Delta K}{dr}\right)_{r=0} = 0. \tag{5A}$$

For the limiting case in which the connective tissue sheath offers no significant diffusion barrier,

$$(\Delta K)_{r=a} = 0. \tag{6A}$$

The other extreme limiting case is considered in the Discussion. Now let J_K° represent the net K density (μA/cm^2) when $\Delta K = 0$, For small perturbations in concentration, variations in J_K will be proportional to ΔK. Thus,

$$J_K = J_K^\circ + B\Delta K \quad \text{where} \quad B \equiv \left(\frac{dJ_K}{dK}\right)_{K=0}. \tag{7A}$$

In general B will be negative (see Fig. 6). Substituting (7A) into (4A),

$$\frac{d^2\Delta K}{dr^2} - \left(\frac{-2B}{wFD}\right)\Delta K = \frac{-2}{wFD}J_K^\circ. \tag{8A}$$

Now let $\lambda_K = (-2B/wFD)^{-1/2}$. The solution of (8A) which satisfies the boundary conditions (5A) and (6A) is

$$\Delta K = \frac{J_K^\circ}{B}\left[\frac{\cosh(r/\lambda_K)}{\cosh(a/\lambda_K)} - 1\right]. \tag{9A}$$

This expression for ΔK has the same form as the equation for the voltage difference

ΔV between cleft membrane potential $V(r)$ and an applied surface membrane potential $V(a)$. Rewriting eqn. (6A) from the paper by Schoenberg *et al.* (1975),

$$\Delta V = V(r) - V(a) = V(a)\left[\frac{\cosh(r/\lambda_c)}{\cosh(a/\lambda_a)} - 1\right]. \tag{10A}$$

Here λ_c, the electrical space constant in the radial direction is given by

$$\lambda_c = \sqrt{\frac{wR'_m}{2R_e}}, \tag{11A}$$

where R'_m is the cleft membrane resistance and R_e is the cleft lumen resistivity.

Fig. 7 illustrates the radial K profile predicted by (9A) for the experiment illustrated in Fig. 6. Values for J_K° and B were obtained by attributing i_o to K current. This seems reasonable since K channels show strong inward rectification over the potentials between -79 and -105 mV, while other currents such as background I_{Na} or I_{Cl} are weakly voltage-dependent (Cohen, Daut & Noble, 1976) and therefore contribute very little to i_o. For the experiment in Fig. 6,

$$J_K^\circ = 2{\cdot}92\ \mu\text{A}.\text{cm}^{-2}, \quad B = -1{\cdot}1\ \text{A}.\text{cm}.\text{mole}^{-1}, \quad a = 52\ \mu\text{m}.$$

Assuming that $w = 1\ \mu$m (Johnson & Sommer, 1967; Sommer & Johnson, 1968),

$$\lambda_K = \sqrt{\frac{wFD}{-2B}} = 100{\cdot}4\ \mu\text{m}.$$

As Fig. 7 indicates, the K profile is shallow for this value of λ_K, and dips to a minimum concentration of 3·68 mM at the centre of the prepraration. For the cleft width of 300Å, λ_K drops to 17·4 μm, the radial profile becomes much more bowed, and the axial concentration falls to 1·6 mM. Calculations for narrow clefts give only a rough idea of the behaviour of sheep Purkinje fibres since (7A) and other considerations become much more approximate as the depletion becomes large.

A spatially average K depletion, $\overline{\Delta K}$ can be determined from (9A) by integrating ΔK over the length of the cleft.

$$\overline{\Delta K} = \frac{1}{a}\int_0^a \Delta K \,.\, \mathrm{d}r = \frac{J_K^\circ}{B}\left[\frac{\lambda}{a}\tanh\left(\frac{a}{\lambda}\right) - 1\right]. \tag{12A}$$

For the 1 μm cleft, $\overline{\Delta K} = -0{\cdot}21$ mM, while for the 300 Å cleft, $\overline{\Delta K} = -1.77$ mM.

Relation between $\overline{\Delta K}$ and depletion current

The relationship between K depletion and the apparent depletion current i_d can be expressed in a general way which does not depend on a specific cleft model. If the local depletion current is linearly related to the local fall in cleft K concentration, $\Delta J_K(r) = B\Delta K(r)$, then

$$\overline{\Delta J_K} = B\overline{\Delta K}, \tag{13A}$$

where the horizontal bar denotes a spatial average over the fibre cross-section. Letting A_c denote the cleft membrane area,

$$i_d = A_c\,\overline{\Delta J_K} = A_c\,B\overline{\Delta K} \tag{14A}$$

If as before we approximate $B \equiv (dJ_K/dK)_{K=K_0}$ by $(di_o/dK)/A_t$, where A_t is the local membrane area,

$$i_d = \frac{A_c}{A_t}\left(\frac{di_o}{dK}\right)\overline{\Delta K}. \tag{15A}$$

Eqn. (15A) does not depend upon assumptions about w or D. It is used on p. 237 to calculate $\overline{\Delta K}$ from i_d. In the example given in Fig. 6, the total area A_t was estimated by dividing the total capacitance (0·0154 μF) by 1 μF/cm^2. The area of the clefts A_c was then approximated by subtracting the apparent cylindrical area of the cell core ($2{\cdot}82 \times 10^{-3}$ cm^2) without correction for membrane folding (cf. Schoenberg *et al.* 1975). Thus

$$\frac{A_c}{A_t} = \frac{0{\cdot}0154 - 0{\cdot}00282}{0{\cdot}0154} = 0{\cdot}81.$$

The estimate A_c/A_t would fall to 0·67 if one assumed that the surface membrane were folded by a factor of 1·8 as in sheep Purkinje fibre (Mobley & Page, 1972).

Depletion currents predicted from cleft model

Now the general relation between $\overline{\Delta K}$ and i_d can be applied to the specific cleft model developed earlier. Combining (12A) and (15A) gives

$$\frac{i_d}{i_o} = \frac{A_c}{A_t}\left[\frac{\lambda}{a}\tanh\left(\frac{a}{\lambda}\right) - 1\right]. \tag{16A}$$

For the 1 μm cleft, (16A) predicts $i_d/i_o = 6{\cdot}5\,\%$. For the 300Å cleft, the predicted $i_d/i_o = 54\,\%$.

We thank Dr Edward A. Johnson for suggesting that we study rabbit Purkinje fibres, Dr Steven Siegelbaum for extensive collaboration in the earlier stages of this project, and Mr Daniel Biemesderfer for providing light and electron micrographs of rabbit Purkinje preparations. This work was supported by grant HL 13306 from the U.S. Public Health Service and an Established Investigatorship from the American Heart Association.

REFERENCES

ADRIAN, R. H. & ALMERS, W. (1974). Membrane capacity measurements on frog skeletal muscle in media of low ionic content. *J. Physiol.* **237**, 573–605.

ARONSON, R. S. & GELLES, J. M. (1977). The effect of ouabain, dinitrophenol, and lithium on the pacemaker current in sheep cardiac Purkinje fibres. *Circulation Res.* **40**, 517–524.

ATTWELL, D. & COHEN, I. (1977). The voltage clamp of multicellular preparations. *Prog. Biophys. molec. Biol.* **31**, 201–245.

BARR, L., HEADINGS, V. E. & BOHR, D. F. (1962). Potassium and the recovery of arterial smooth muscle after cold storage. *J. gen. Physiol.* **46**, 19–33.

BARRY, P. H. & ADRIAN, R. H. (1973). Slow conductance changes due to potassium depletion in the transverse tubules of frog skeletal muscle during hyperpolarizing pulses. *J. membrane Biol.* **14**, 243–292.

BAUMGARTEN, C. M. & ISENBERG, G. (1977). Depletion and accumulation of potassium in the extracellular clefts of cardiac Purkinje fibres during voltage clamp hyperpolarization and depolarization. *Pflügers Arch.* **368**, 19–31.

BAUMGARTEN, C. M., ISENBERG, G., MCDONALD, T. F. & TEN EICK, R. E. (1977). Depletion and accumulation of potassium in the extracellular clefts of cardiac Purkinje fibres during voltage

clamp hyperpolarization and depolarization. Experiments in Na-free bathing media. *J. gen. Physiol.* **70**, 149–169.

BEELER, G. W., JR. & REUTER, H. (1970). Voltage clamp experiments on ventricular myocardial fibres. *J. Physiol.* **207**, 165–190.

CLEEMANN, L. & MORAD, M. (1976). Extracellular potassium accumulation and inward-going potassium rectification in voltage clamped ventricular muscle. *Science, N.Y.* **191**, 90–92.

COHEN, I., DAUT, J. & NOBLE, D. (1976). The effects of potassium and temperature on the pacemaker current, I_{K_2} in Purkinje fibres. *J. Physiol.* **260**, 55–74.

COLATSKY, T. J., SIEGELBAUM, S. A. & TSIEN, R. W. (1978). Electrical evidence for wide clefts in voltage clamped rabbit Purkinje fibres. Presence of slow inward current. *Biophys. J.* **21**, 56*a*.

CONNOR, J., BARR, L. & JAKOBSSON, E. (1975). Electrical characteristics of frog atrial trabeculae in the double sucrose gap. *Biophys. J.* **15**, 1047–1067.

CORABOEUF, E. & WEIDMANN, S. (1954). Temperature effects on the electrical activity of Purkinje fibres. *Helv. physiol. pharmac. Acta* **12**, 32–41.

CRANEFIELD, P. F. (1975). *The Conduction of the Cardiac Impulse.* Mount Kisco, New York: Futura.

DECK, K. A., KERN, R. & TRAUTWEIN, W. (1964). Voltage clamp technique in mammalian cardiac fibres. *Pflügers Arch. ges. Physiol.* **280**, 50–62.

DEMELLO, W. C. (1972). The healing-over process in cardiac and other muscle fibres. In *Electrical Phenomena in the Heart*, ed. DEMELLO, W. C., pp. 335–395. New York: Academic.

DRAPER, M. H. & WEIDMANN, S. (1951). Cardiac resting and action potentials recorded with an intracellular electrode. *J. Physiol.* **115**, 74–94.

DUDEL, J., PEPER, K., RÜDEL, R. & TRAUTWEIN, W. (1967). The dynamic chloride component of membrane current in Purkinje fibres. *Pflügers Arch. ges. Physiol.* **295**, 197–212.

FALK, G. & FATT, P. (1964). Linear electrical properties of striated muscle fibres observed with intracellular electrodes. *Proc. R. Soc.* B. **160**, 69–123.

FERRIER, G. R. (1977). Digitalis arrhythmias: role of oscillatory afterpotentials. *Prog. cardiovasc. Dis.* **19**, 459–474.

FLECKENSTEIN, A. (1977). Specific pharmacology of calcium in myocardium, cardiac pacemakers, and vascular smooth muscle. *Annu. Rev. Pharmacol. & Toxicol.* **17**, 149–166.

FOZZARD, H. A. (1966). Membrane capacity of the cardiac Purkinje fibre. *J. Physiol.* **182**, 255–267.

FOZZARD, H. A. & BEELER, G. W., Jr. (1975). The voltage clamp and cardiac electrophysiology. *Circulation Res.* **37**, 403–413.

FOZZARD, H. A. & HIRAOKA, M. (1973). The positive dynamic current and its inactivation properties in cardiac Purkinje fibres. *J. Physiol.* **234**, 569–586.

FRANEKENHAEUSER, B. & HODGKIN, A. L. (1956). The after-effects of impulses in the giant nerve fibres of *Loligo*. *J. Physiol.* **131**, 341–376.

FREYGANG, W. H. & TRAUTWEIN, W. (1970). The structural implications of the linear electrical properties of cardiac Purkinje strands. *J. gen. Physiol.* **55**, 524–547.

GIBBS, C. L. & JOHNSON, E. A. (1961). Effect of changes in frequency of stimulation upon rabbit ventricular action potential. *Circulation Res.* **9**, 165–170.

HARRINGTON, L. & JOHNSON, E. A. (1973). Voltage clamp of cardiac muscle in a double sucrose gap. A feasibility study. *Biophys. J.* **13**, 626–647.

HAUSWIRTH, O., NOBLE, D. & TSIEN, R. W. (1969). The mechanism of oscillatory activity at low membrane potentials in cardiac Purkinje fibres. *J. Physiol.* **200**, 255–265.

HELLAM, D. C. & STUDT, J. W. (1974). A core-conductor model of the cardiac Purkinje fibre based on structural analysis. *J. Physiol.* **243**, 637–660.

DE HEMPTINNE, A. (1973). The double sucrose gap as a method to study the electrical properties of heart cells. *Eur. J. Cardiol.* **1/2**, 157–162.

HOFFMAN, B. F. & CRANEFIELD, P. F. (1960). *Electrophysiology of the Heart*, New York: McGraw-Hill.

JACK, J. J. B., NOBLE, D. & TSIEN, R. W. (1975). *Electric Current Flow in Excitable Cells.* Oxford: Oxford University Press.

JOHNSON, E. A. & LIEBERMAN, M. (1971). Heart: excitation and contraction. *A. Rev. Physiol.* **33**, 479–532.

JOHNSON, E. A. & SOMMER, J. R. (1967). A strand of cardiac muscle. Its ultrastructure and the electrophysiological implications of its geometry. *J. cell Biol.* **33**, 103–129.

JOHNSON, E. A. & TILLE, J. (1961). Investigations of the electrical properties of cardiac muscle fibres with the aid of intracellular double-barrelled electrodes. *J. gen. Physiol.* **44**, 443–467.

KASS, R. S., LEDERER, W. J., TSIEN, R. W. & WEINGART, R. (1978). Role of calcium ions in transient inward currents and aftercontractions induced by strophanthidin in cardiac Purkinje fibres. *J. Physiol.* **281**, 187–208.

KASS, R. S., SIEGELBAUM, S. A. & TSIEN, R. W. (1976). Incomplete inactivation of the slow inward current in cardiac Purkinje fibres. *J. Physiol.* **263**, 127–128*P*.

KASS, R. S., SIEGELBAUM, S. A. & TSIEN, R. W. (1978). Can slow inward current be adequately voltage clamped in cardiac Purkinje fibres? *Biophys. J.* **21**, 56*a*.

KASS, R. S. & TSIEN, R. W. (1976). Analysis of the three microelectrode method as applied to inward currents in cardiac Purkinje fibres. *Biophys. J.* **15**, 257*a*.

KENYON, J. L. & GIBBONS, W. R. (1979). 4-Aminopyridine and the early outward current of sheep cardiac Purkinje fibres. *J. gen. Physiol.* (in the Press).

KUNZE, D. L. (1977). Rate-dependent changes in extracellular potassium in the rabbit atrium. *Circulation Res.* **41**, 122–127.

LEDERER, W. J. & TSIEN, R. W. (1976). Transient inward current underlying arrhythmogenic effects of cardiotonic steroids in Purkinje fibres. *J. Physiol.* **263**, 73–100.

LIEBERMAN, J., SAWANOBORI, T., KOOTSEY, J. M., & JOHNSON, E. A. (1975). A synthetic strand of cardiac muscle. Its passive electrical properties. *J. gen. Physiol.* **65**, 527–550.

MCALLISTER, R. E., NOBLE, D. & TSIEN, R. W. (1975). Reconstruction of the electrical activity of cardiac Purkinje fibres. *J. Physiol.* **251**, 1–59.

MCGUIGAN, J. A. (1974). Some limitations of the double sucrose gap, and its use in a study of the slow outward current in mammalian ventricular muscle. *J. Physiol.* **240**, 775–806.

MACDONALD, R. L., HSU, D., MANN, J. E., JR. & SPERELAKIS, N. (1975). An analysis of the problem of K^+ accumulation in the intercalated disk clefts of cardiac muscle. *J. theor. Biol.* **51**, 455–473.

MAUGHAN, D. W. (1973). Some effects of prolonged polarization on membrane currents in bullfrog atrial muscle. *J. Membrane Biol.* **11**, 331–352.

MEHDI, T. & SACHS, F. (1978). Voltage clamp of isolated cardiac Purkinje cells. *Biophys. J.* **21**, 165*a*.

MOBLEY, B. A. & PAGE, E. (1972). The surface area of sheep cardiac Purkinje fibres. *J. Physiol.* **200**, 547–563.

NOBLE, D. & TSIEN, R. W. (1969). Outward membrane currents activated in the plateau range of potentials in cardiac Purkinje fibres. *J. Physiol.* **200**, 205–231.

NOBLE, D. (1975). *The Initiation of the Heartbeat.* Oxford University Press.

NOBLE, S. J. (1976). Potassium accumulation and depletion in frog atrial muscle. *J. Physiol.* **258**, 579–613.

PAGE, E. (1978). Quantitative ultrastructural analysis in cardiac membrane physiology. *Am. J. Physiol.* **235**, C147–C158.

PAGE, S. G. & NIEDERGERKE, R. (1972). Structures of physiological interest in the frog heart ventricle. *J. cell. Sci.* **11**, 179–203.

REUTER, H. (1968). Slow inactivation of currents in cardiac Purkinje fibres. *J. Physiol.* **197**, 233–253.

REUTER, H. (1973). Divalent cations as charge carriers in excitable membranes. *Prog. Biophys. molec. Biol.* **26**, 1–43.

SACHS, F. (1975). Electrophysiological properties of tissue cultured heart cells grown in a linear array. *J. Membrane Biol.* **28**, 373–399.

SCHNEIDER, M. F. & CHANDLER, W. K. (1976). Effects of membrane potential on the capacitance of skeletal muscle fibers. *J. gen. Physiol.* **67**, 125–163.

SCHOENBERG, M., DOMINGUEZ, G. & FOZZARD, H. A. (1975). Effect of diameter on membrane capacity and conductance of sheep cardiac Purkinje fibers. *J. gen. Physiol.* **65**, 441–458.

SOMMER, J. R. & JOHNSON, E. A. (1968). Cardiac muscle. A comparative study in Purkinje fibres and ventricular fibres. *J. cell Biol.* **36**, 497–526.

THOMPSON, S. M. (1975). Na^+ channel permeability to metallic and organic cations in the voltage clamped *trabeculae carneae cordis* of the rabbit heart. Ph.D. Thesis, University of Iowa.

TILLE, J. (1966). Electrotonic interaction between muscle fibres in the rabbit ventricle. *J. gen. Physiol.* **50**, 189–202.

TSIEN, R. W. (1974). Effects of epinephrine on the pacemaker potassium current of cardiac Purkinje fibres. *J. gen. Physiol.* **64**, 320–342.

TSIEN, R. W. & CARPENTER, D. O. (1978). Ionic mechanisms of pacemaker activity in cardiac Purkinje fibres. *Fedn Proc.* **37**, 2127–2131.

VASSALLE, M. (1966). Analysis of cardiac pacemaker potential using a 'voltage clamp' technique. *Am. J. Physiol.* **210**, 1335–1341.

VEREECKE, J. & CARMELIET, E. (1971). Sr action potentials in cardiac Purkinje fibres. I. Evidence for a regenerative increase in Sr conductance. *Pflügers Arch.* **322**, 60–72.

WEIDMANN, S. (1952). The electrical constants of Purkinje fibres. *J. Physiol.* **118**, 348–360.

WEIDMANN, S. (1955). The effect of the cardiac membrane potential on the rapid availability of the sodium-carrying system. *J. Physiol.* **127**, 213–224.

WEIDMANN, S. (1966). The diffusion of radiopotassium across intercalated disks of mammalian cardiac muscle. *J. Physiol.* **187**, 323–342.

WEIDMANN, S. (1970). Electrical constants of trabecular muscle from mammalian heart. *J. Physiol.* **210**, 1041–1054.